

# Role of initial conditions in 1D diffusive systems: compressibility, hyperuniformity and long-term memory

Tirthankar Banerjee,<sup>1,\*</sup> Robert L. Jack,<sup>1,2</sup> and Michael E. Cates<sup>1</sup>

<sup>1</sup>*DAMTP, Centre for Mathematical Sciences, University of Cambridge, Wilberforce Road, Cambridge, CB3 0WA*

<sup>2</sup>*Yusuf Hamied Department of Chemistry, University of Cambridge, Lensfield Road, Cambridge CB2 1EW, United Kingdom*

(Dated: June 20, 2022)

We analyse the long-lasting effects of initial conditions on fluctuations in one-dimensional diffusive systems. We consider both the fluctuations of current for non-interacting diffusive particles starting from a step-like initial density profile, and the mean-square displacement of tracers in homogeneous systems with single-file diffusion. For these two cases, we show analytically (via the propagator and Macroscopic Fluctuation Theory, respectively) that the long-term memory of initial conditions is mediated by a single static quantity: a generalized compressibility that quantifies the density fluctuations of the initial state. We thereby identify a universality class of hyperuniform initial states whose dynamical variances coincide with the ‘quenched’ cases studied previously; we also describe a continuous family of other classes among which equilibrated (or ‘annealed’) initial conditions are but one family member. We verify our predictions through extensive Monte Carlo simulations.

Many physical systems are ergodic: independent of their initial preparation, they relax to steady states whose properties can then be analysed with standard tools of statistical mechanics [1]. Non-ergodicity, a signature of memory effects [2–5], can arise when phase transitions lead to systems with non-unique steady states [6–9]. However, a separate class of non-ergodicity occurs in systems that lack any steady state [10, 11]. For example, suppose that particles are initialised at fixed density to the left of some arbitrary origin, and allowed to diffuse independently [10, 12]. The particles then spread throughout space, but never reach steady state; the system remains far from equilibrium indefinitely. In such types of non-ergodicity, the initialisation procedure of the system can have an everlasting effect on its future behaviour [10, 12]. Despite their simple setups, the mechanisms of such long-term memory effects remain far from fully understood. An interesting effect of initialisation – present in the example above and in more complex systems [13–18] – is that for arbitrarily large times, variances of dynamical quantities depend on the initial conditions, which might be randomly sampled from the stationary dynamics, or fixed in a specific configuration (for example, equi-spaced). By analogy with spin-glass physics [19], one may also distinguish annealed variances (where dynamical fluctuations and random initial conditions are treated on an equal footing), and quenched variances (which measure the dynamical fluctuations associated with a typical initial condition) [10].

In the systems studied here, the quenched variance coincides with the dynamical variance obtained for equi-spaced initial conditions [14]. Previous works [10, 12, 15, 16] highlighted differences between quenched and annealed variances, for initial states that are sampled from the stationary distribution of the model dynamics. In this work, we analyse the dependence of dynamical fluctuations on a much wider range of initial conditions, for

two classes of one dimensional (1D) diffusive systems. In particular, we show that (i) the dependence of dynamical variances on the initial state can be captured by a single number, encoding its long-wavelength density fluctuations; (ii) the relaxation dynamics of these fluctuations is the sole origin of persistent memory effects; and (iii) the existing “quenched” and “annealed” results of [10, 12, 15] become two special cases within a continuous family.

We now summarize our main results, before presenting their derivation. First, consider non-interacting particles with all particles initially to the left of an arbitrary origin in 1D, such that the density has a step-like profile. If the long-time behavior of the particles is diffusive, then for large times  $T$ , we show that the variance of the (time-integrated) particle flux  $Q(T)$  through the origin is

$$\text{Var}[Q(T)] \simeq \Delta Q_{\text{noise}}^2(T) + \alpha_{\text{ic}} \Delta Q_{\text{dens}}^2(T). \quad (1)$$

Here  $\Delta Q_{\text{noise}}^2$  is a purely dynamical contribution; the remainder depends on the initial condition. Detailed formulae are given below, but the central observation is that this dependence is fully determined by a single number

$$\alpha_{\text{ic}} = \lim_{\ell \rightarrow \infty} \frac{\text{Var}[n(\ell)]}{\langle n(\ell) \rangle} \quad (2)$$

where  $n(\ell)$  is the number of particles that are initially found within a distance  $\ell$  of the origin. Notably, (1,2) link two quantities that are experimentally accessible (*e.g.*, via microscopy) without knowing the interaction details [20–22]. If the initial condition is a thermal equilibrium state,  $\alpha_{\text{ic}}$  is proportional to the compressibility [23, 24]. Importantly, however, the initial condition need not be thermal, nor even a stationary (‘annealed’) state of the chosen dynamics. We identify  $\alpha_{\text{ic}}$  more generally as a Fano factor [25], which is familiar from analyses of hyperuniform (HU) states, which have  $\alpha_{\text{ic}} = 0$ , by definition [26]. Physically, (1) shows that the everlasting effect

of the initial condition is fully encoded in its large-scale density fluctuations whose relaxation times are arbitrarily long. All HU initial conditions lead to the same result for  $\text{Var}[Q(T)]$ , which also coincides with the quenched variance of [10, 12]: this is an unexpectedly universal result. In contrast, the ‘annealed’ variance of [10, 12] becomes one member of a continuous family, indexed only by  $\alpha_{\text{ic}}$ .

Our second example involves the single-file diffusion [14, 15, 27–33] of a homogeneous interacting particle system under conditions where Macroscopic Fluctuation Theory (MFT) is applicable [15, 34–40]. Identifying a single tracer particle starting from the origin, we show that the variance of its position  $X(T)$  satisfies

$$\text{Var}[X(T)] \simeq \Delta X_{\text{noise}}^2(T) + \alpha_{\text{ic}} \Delta X_{\text{dens}}^2(T), \quad (3)$$

for large times  $T$ , where again the dependence on the initial condition is fully controlled by  $\alpha_{\text{ic}}$ , independent of the dynamics. These dynamics now may include complex interactions, but the same physical mechanism is at work. Equation 3 signifies that for all MFT compliant dynamics, the mean-squared displacement comprises a purely dynamical contribution, plus a part that depends on the (arbitrary) initial state purely via  $\alpha_{\text{ic}}$ . Although the connection of compressibility to hardcore tracer motion was noted in a less general setting [17, 41], Eq. (3) goes far beyond previous results for ‘equilibrated’ initial states [15, 42–44].

We now outline the derivation of these results, focussing on the physical mechanism. We greatly generalize the results of previous studies [10, 12, 14–16, 41–45] and explain the special status of HU initial conditions.

*Current fluctuations for non-interacting particles:* Consider non-interacting particles with initial positions  $\mathbf{y} = (y_1, y_2, \dots)$  lying to the left of the origin ( $y_i < 0$ ) [12]. At time  $t$ , define  $\chi_i(t) = 1$  if particle  $i$  has position  $x_i(t) > 0$ , and  $\chi_i(t) = 0$  otherwise. Also define the propagator  $G(x, y, t)$  as the probability density that a particle is at position  $x$ , given that it was at position  $y$  a time  $t$  earlier. For given initial conditions  $\mathbf{y}$ , we have  $\langle \chi_i(t) \rangle_{\mathbf{y}} = U(-y_i, t)$ , where

$$U(z, t) = \int_0^\infty dx G(x, -z, t). \quad (4)$$

The mean integrated flux through the origin is then obtained by summing over all particles:  $\langle Q(t) \rangle_{\mathbf{y}} = \sum_i U(-y_i, t)$ . Defining the empirical density of the initial condition as  $\hat{\rho}(x|\mathbf{y}) = \sum_i \delta(x - y_i)$ , we now write

$$\langle Q(t) \rangle_{\mathbf{y}} = \int_0^\infty dz \hat{\rho}(-z|\mathbf{y}) U(z, t) \quad (5)$$

Here and in the following, positive values of  $z$  represent initial positions to the *left* of the origin.

Since the particles are non-interacting and  $\chi_i \in \{0, 1\}$ , the variance of the flux is

$$\langle Q(t)^2 \rangle_{\mathbf{y}} - \langle Q(t) \rangle_{\mathbf{y}}^2 = \int_0^\infty dz \hat{\rho}(-z|\mathbf{y}) U(z, t) [1 - U(z, t)]. \quad (6)$$

This is a purely dynamical quantity for given initial condition  $\mathbf{y}$ . Now averaging further over  $\mathbf{y}$  (denoted as  $\overline{(\dots)}$ ), the final variance of the flux is [6, 7]

$$\text{Var}[Q(t)] = \Delta Q_{\text{noise}}^2(t) + \Delta Q_{\text{ic}}^2(t) \quad (7)$$

where

$$\begin{aligned} \Delta Q_{\text{noise}}^2 &= \overline{\langle Q(t)^2 \rangle_{\mathbf{y}}} - \overline{\langle Q(t) \rangle_{\mathbf{y}}^2} \\ \Delta Q_{\text{ic}}^2(t) &= \overline{\langle Q(t) \rangle_{\mathbf{y}}^2} - \overline{Q(t)}_{\mathbf{y}}^2 \end{aligned} \quad (8)$$

are contributions from fluctuations in the dynamics and in the initial condition, respectively. By definition,  $\Delta Q_{\text{noise}}^2$  is a quenched variance. Formally,  $\text{Var}[Q(t)]$  is always obtained by an annealed calculation, but we reserve the term ‘annealed’ in this work for the specific case where the correlations in the initial state are inherited from the stationary state of the model, as in [10, 12]. Using (5) yields

$$\Delta Q_{\text{ic}}^2(t) = \int_0^\infty \int_0^\infty dz dz' U(z, t) U(z', t) C_2(z, z') \quad (9)$$

where  $C_2(z, z') = \overline{\hat{\rho}(-z|\mathbf{y}) \hat{\rho}(-z'|\mathbf{y})} - \overline{\hat{\rho}(-z|\mathbf{y})} \overline{\hat{\rho}(-z'|\mathbf{y})}$ . Hence, the initial conditions enter the variance through the one- and two-point correlations of the density only.

So far, this analysis is general: we now make several assumptions on the system of interest. First, assume that for large times  $t$ , the propagator  $G$  is Gaussian with diffusion constant  $D$ , so that

$$U(z, t) \simeq \frac{1}{2} \text{erfc} \left[ \frac{z}{\sqrt{4Dt}} \right] \quad \text{as } t \rightarrow \infty, \quad (10)$$

with  $\text{erfc}(x)$  being the complementary error function. This assumption includes passive diffusers, and many kinds of active particle (see below). Second, we assume that the initial conditions arise by taking an infinite, translationally invariant system and erasing all particles to the right of the origin. This means that  $\hat{\rho}(-z|\mathbf{y}) = \bar{\rho} \Theta(z)$  and  $C_2(z, z') = \bar{\rho} \Theta(z) \Theta(z') C(z - z')$  where  $\Theta(z)$  is the Heaviside function and  $C(z - z')$  the two-point correlator before erasure. This assumption can be relaxed, but already reveals the behavior of interest here.

At large times,  $T$ , (9) and (10) then yield

$$\begin{aligned} \Delta Q_{\text{ic}}^2(T) &= \frac{\bar{\rho} \sqrt{DT}}{4\pi} \int_0^\infty dy \int_0^\infty dy' \int_{-\infty}^\infty dp e^{ip(y'-y)} \\ &\quad \times S \left( \frac{p}{\sqrt{4DT}} \right) \text{erfc}(y) \text{erfc}(y'). \end{aligned} \quad (11)$$

where  $S(q) = \int_{-\infty}^{\infty} dz C(z) e^{-iqz}$  is the structure factor. The initial condition enters this expression through the single number  $\alpha_{ic} = \lim_{q \rightarrow 0} S(q)$ , which coincides with the asymptotic variance (2) [1, 24, 46]. Replacing the structure factor by its limit, the integrals in (11) yield  $\Delta Q_{ic}^2(T) = \alpha_{ic} \Delta Q_{dens}^2(T)$  with

$$\Delta Q_{dens}^2(T) \simeq (\sqrt{2} - 1) \sqrt{\frac{\bar{\rho}^2 DT}{2\pi}}. \quad (12)$$

Similarly using (6),  $\Delta Q_{noise}^2$  is:

$$\Delta Q_{noise}^2(T) \simeq \sqrt{\frac{\bar{\rho}^2 DT}{2\pi}}. \quad (13)$$

Combining (7,12,13) yields explicit expressions for all terms in (1); initial conditions enter only through  $\alpha_{ic}$ .

We now interpret these results. This  $\Delta Q_{noise}^2$  is the quenched variance of [10, 12]. Our Eq. (13) shows that the total variance coincides with the quenched result for *any* HU initial state, because these all have  $\alpha_{ic} = 0$ . The ‘annealed’ result of [10, 12] is obtained by taking  $C(z) = \delta(z)$ , corresponding to the equilibrium state of this model, so  $\alpha_{ic} = 1$ . This result is larger than the quenched variance by a factor  $\sqrt{2}$ . Remarkably, these quenched and annealed results can now be identified as two specific choices within an infinite family of initial conditions, fully parameterized by  $\alpha_{ic}$ . Note that our theory extends to  $\alpha_{ic} > 1$ , corresponding to initial states generated, *e.g.*, by equilibrating attractive interactions [46]. However, we address numerically below only  $\alpha_{ic} \leq 1$  whose initial conditions are more easily generated.

Our results explain the mechanism by which the initial conditions affect the variance. Using (10), the physical meaning of (5) is that particles that start much less than  $\sqrt{4DT}$  from the origin have passed it with probability 1/2, while particles starting much further away are unlikely to have passed it. Hence, the average flux is controlled by the number of particles within  $\sqrt{4DT}$  of the origin: the variance of this number is determined by  $\alpha_{ic}$  [from (2)] and this determines  $\Delta Q_{ic}^2(T)$ . Finally, we attribute the everlasting effect of the initial conditions to the long-wavelength density fluctuations that determine  $\alpha_{ic}$ , whose diverging relaxation times act as the source of long-term memory.

Figure 1(a) shows  $\text{Var}[Q(T)]$  for point Brownian particles with  $D = 1$ , obtained from Monte Carlo (MC) simulations for different values of  $\alpha_{ic}$ , see [46] for details. In the initial state for these numerics, particles are placed at random, with spacings constrained to exceed some constant  $r_0$ : this allows  $\alpha_{ic} = (1 - r_0 \bar{\rho})^2$  to be adjusted between 0 (equal spacing  $r_0 = 1/\bar{\rho}$ ) and unity (ideal gas configuration,  $r_0 = 0$ ) [46]. The results match the predictions (1,12,13). To check that all dependence on the initial conditions comes from  $\alpha_{ic}$ , we also simulated a different HU initial condition ( $\alpha_{ic} = 0$ ) where equi-spaced particles are given independent random displacements of

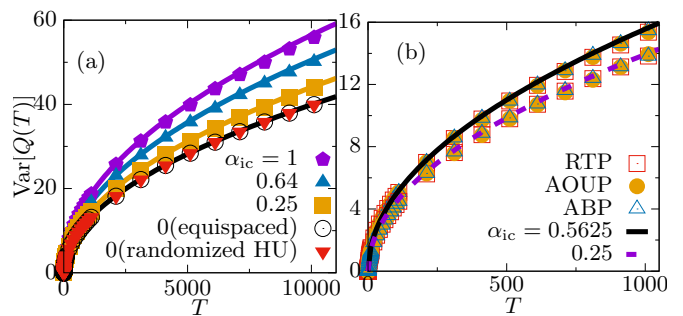


FIG. 1. (a) The variance  $\text{Var}[Q(T)]$  of non-interacting Brownian particles with  $D = 1$  and  $\bar{\rho} = 1$ , at different values of  $\alpha_{ic}$ . The MC simulation results (points) match the theoretical prediction (1) (solid lines). For HU initial states ( $\alpha_{ic} = 0$ ), two different initial setups are shown: equi-spaced initial positions with or without additional random displacements. (b) The variance  $\text{Var}[Q(T)]$  for noninteracting active particles at long times. Points show simulation results; lines are the prediction (1).

a fixed size [46]: the long-time behavior is exactly the same as with equi-spaced initial particles.

Figure 1(b) shows results for three popular models of active particles [47–54]: active Ornstein-Uhlenbeck particles (AOUPs), active Brownian particles (ABPs) and run-and-tumble particles (RTPs), see [46] for details. These systems all satisfy (10) for large times with  $D$  their late-time diffusivity. These systems also precisely obey our predictions (1,12,13).

*Tracer motion in single-file systems:* The previous system of noninteracting particles allows for straightforward calculation and physical interpretation. We now turn to a class of strongly interacting systems, where we predict similar effects. Consider an infinite 1D system of hardcore interacting particles, whose initial condition is homogeneous, with mean density  $\bar{\rho}$  and two-point correlation  $C(z)$  as above. A single tracer particle is identified, and its displacement between times 0 and  $T$  is denoted by  $X(T)$ . We focus on the variance of this quantity: our main result is (3), as we now explain. The physical mechanism for this result is the same as (1), although the computation uses a different method.

Our hardcore particles in 1D move in single file; we assume that their hydrodynamic density field  $\rho$  can be described by the MFT equation [34]

$$\partial_t \rho(x, t) = \partial_x [D(\rho) \partial_x \rho(x, t) + \sqrt{\sigma(\rho)} \eta(x, t)], \quad (14)$$

where  $\sigma(\rho)$  and  $D(\rho)$  are the mobility and diffusivity and  $\eta(x, t)$  is Gaussian spatiotemporal white noise. Examples of such MFT systems include hard Brownian particles [15], and the symmetric simple exclusion process [40].

The computation of the tracer statistics follows previous work [15]; we outline the method, with details in [46]. The moment generating function (MGF) of the tracer position is  $\langle e^{\lambda X(T)} \rangle$ , which can be expressed as a path

integral in the Martin-Siggia-Rose formalism [15]:

$$\langle e^{\lambda X(T)} \rangle = \int \mathcal{D}[\rho(x, t), \hat{\rho}(x, t)] e^{-\mathcal{S}[\rho(x, t), \hat{\rho}(x, t)]}, \quad (15)$$

where  $\hat{\rho}(x, t)$  is a response field, and the action is

$$\mathcal{S}[\rho, \hat{\rho}] = -\lambda X(T) + F[\rho] + \int_0^T dt \int_{-\infty}^{\infty} dx \mathcal{L}(\rho, \hat{\rho}). \quad (16)$$

Here  $F[\rho]$  is the log-probability of the initial condition (see below), and

$$\mathcal{L}(\rho, \hat{\rho}) = \hat{\rho} \partial_t \rho - \frac{\sigma(\rho)}{2} (\partial_x \hat{\rho})^2 + D(\rho) (\partial_x \rho) (\partial_x \hat{\rho}). \quad (17)$$

For single-file motion,  $X(T)$  is fully determined by the dynamics of the density: at time  $T$ , all particles between the tracer and the origin must have had initial positions  $y_i < 0$ . This implies [15, 46]

$$\int_0^{X(T)} dx \rho(x, T) = \int_0^{\infty} dx [\rho(x, T) - \rho(x, 0)]. \quad (18)$$

On long enough (hydrodynamic) time scales, noise effects become weak and (15) can be evaluated by a saddle-point method. Physically, this involves the computation of an instanton that generates a large tracer displacement  $X(T)$ , whose size is determined by the parameter  $\lambda$ . We are interested here in the variance of  $X(T)$ , which means that the computation is required at  $O(\lambda^2)$ . At this level, the instanton dynamics is  $\rho(x, t) \approx \bar{\rho} + \lambda q_1(x, t)$  and  $\hat{\rho}(x, t) \approx \lambda p_1(x, t)$ , where  $p_1, q_1$  are canonically conjugate fields; terms at higher order in  $\lambda$  can be neglected. Within MFT, the log-probability of the initial condition is determined by a function  $g_{ic}$ , as  $F[\rho] = \int_{-\infty}^{\infty} dx g_{ic}(\rho(x, 0))$ , which specifies the probability of local density fluctuations [34, 46]. For thermally equilibrated initial conditions,  $g_{ic}$  is related to the free energy; more generally, it is a large-deviation rate function. We emphasise that  $\rho$  is the hydrodynamic density: there may be density correlations on the scale of the interparticle spacing, but  $g_{ic}$  is still a local function of  $\rho$ . Since the density fluctuations are of order  $\lambda$ , it is consistent to approximate [34, 46]

$$g_{ic}(\rho) \approx [\rho(x, 0) - \bar{\rho}]^2 / (2\alpha_{ic}\bar{\rho}) \quad (19)$$

where  $\alpha_{ic} = 1/(\bar{\rho} g_{ic}''(\bar{\rho}))$  is the Fano factor defined in (2). Note that the quenched variance of [15] is equivalent to taking  $\rho(x, 0) = \bar{\rho}$  exactly: this corresponds to  $\alpha_{ic} \rightarrow 0$ . The ‘annealed’ case of an equilibrated initial condition requires  $g_{ic}''(\bar{\rho}) = 2D(\bar{\rho})/\sigma(\bar{\rho})$  which is a fluctuation-dissipation theorem (FDT) [34]. Hence our formalism addresses both known initial conditions on an equal footing, extending the results to a much wider class that includes initial states sampled neither from the systems’ own equilibrium dynamics, nor any other.

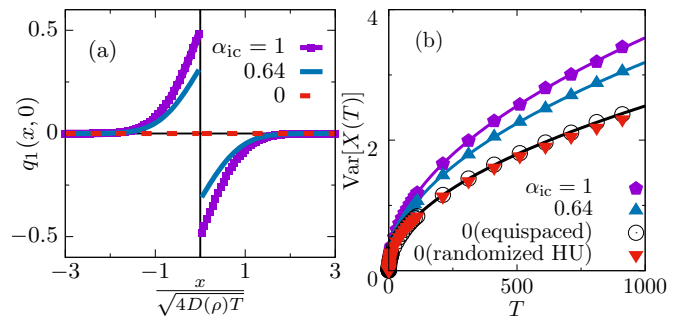


FIG. 2. (a) The non-typical initial condition  $q_1(x, 0)$  that appears when considering fluctuations of  $X(T)$  for various  $\alpha_{ic}$ . Large currents correspond to an excess of particles to the left of the origin, biasing the tracer to the right. (b) The mean-square tracer displacement  $\text{Var}[X(T)]$  in a system of point Brownian particles at density  $\bar{\rho} = 10$ . Numerical results are shown as points; solid lines show the theoretical prediction (26). We show results for two different HU initial conditions, with initialisation protocols the same as Fig. 1.

The instanton dynamics is obtained by extremising the action, leading to

$$\begin{aligned} \partial_t q_1(x, t) &= \partial_x [D(\bar{\rho}) \partial_x q_1(x, t) - \sigma(\bar{\rho}) \partial_x p_1(x, t)] \\ \partial_t p_1(x, t) &= -D(\bar{\rho}) \partial_{xx} p_1(x, t), \end{aligned} \quad (20)$$

with boundary conditions [46]

$$q_1(x, 0) = \bar{\rho} \alpha_{ic} [p_1(x, 0) - p_1(x, T)] \quad (21)$$

$$p_1(x, T) = \Theta(x)/\bar{\rho}. \quad (22)$$

The equations for  $p_1$  are closed and exactly solvable, following [15]. Hence (21) sets the initial condition for the instanton, which is the fluctuation of the initial condition  $\rho(x, 0)$  associated with the prescribed fluctuation of  $X(T)$ :

$$q_1(x, 0) = \alpha_{ic} \left[ \frac{1}{2} \text{erfc} \left( \frac{-x}{\sqrt{4D(\bar{\rho})T}} \right) - \Theta(x) \right]. \quad (23)$$

This result is shown in Fig. 2(a). In physical terms, if the initial density is large on the left of the tracer, then it tends to move to the right, and vice versa. The size of the fluctuation is proportional to  $\alpha_{ic}$  (vanishing for HU initial conditions, which lack these large-scale density fluctuations); the associated length scale is  $\sqrt{4D(\bar{\rho})T}$ . As for the current fluctuations in the non-interacting system considered earlier, this shows that fluctuations of tracer position are strongly coupled to the number of particles within this distance on either side of the origin.

Finally, observe that the variance of the tracer position can be obtained as the second derivative of the MGF.

Following [15], one obtains (3) with

$$\Delta X_{\text{noise}}^2(T) \simeq \frac{1}{\bar{\rho}} \sqrt{\frac{\sigma(\bar{\rho})^2 T}{2\pi \bar{\rho}^2 D(\bar{\rho})}}, \quad (24)$$

$$\Delta X_{\text{dens}}^2(T) \simeq \frac{\sqrt{2}-1}{\bar{\rho}} \sqrt{\frac{2D(\bar{\rho})T}{\pi}}. \quad (25)$$

For the specific case of hard Brownian particles with diffusion constant  $D$ , one also has  $\sigma(\bar{\rho}) = 2D\bar{\rho}$  and  $D(\bar{\rho}) = D$ . Hence,

$$\text{Var}[X(T)] \simeq \frac{1}{\bar{\rho}} \sqrt{\frac{2DT}{\pi}} \left[ 1 + \alpha_{\text{ic}}(\sqrt{2}-1) \right]. \quad (26)$$

This result is verified numerically in Fig. 2(b), for three different values of  $\alpha_{\text{ic}}$  with  $D = 1, \bar{\rho} = 10$ . For the HU case ( $\alpha_{\text{ic}} = 0$ ), we also show that two different initial preparations yield the same result, similarly to Fig. 1.

To summarise, we have considered two different situations where the initial preparation of a 1D diffusive system has long-lasting effects on fluctuations of dynamical quantities. We showed that this dependence is captured by the single parameter  $\alpha_{\text{ic}}$ , which quantifies large-scale density fluctuations in the initial state. This quantity emphasises the special role of HU initial states, as those which minimise these long-lived fluctuations. All HU initial states form a single universality class, for which the flux variance and the tracer mean-squared displacement match previous ‘quenched’ results [10, 12, 15]. In contrast, the ‘annealed’ case (sampling the initial state from the stationary or equilibrated dynamics) is just one member of a continuous family of distinct classes of initial conditions, parameterised by  $\alpha_{\text{ic}}$ . In all these classes, long-term memory stems from the unlimited decay times of long length-scale density inhomogeneities; the fluctuations at time  $T$  are controlled by the number of particles that started within  $\sqrt{4DT}$  of the origin.

Analogous discrepancies between quenched and annealed results for different types of initial states, e.g., [16, 17], should broadly share the mechanism elucidated here. Our results are limited to variances of dynamical quantities: higher moments (and large deviations) of these quantities presumably depend on higher-order statistics of the initial density, opening up rich new possibilities. There are further open questions around the behaviour of those single-file systems that lie beyond the scope of MFT [55], and for driven 1D systems [45, 56–59]. Beyond 1D, our results may prove relevant to anisotropic effects seen in higher dimensions [60–62].

*Acknowledgments:* We thank Camille Scalliet, Johannes Pausch and Jean-François Derivaux for helpful discussions. Work funded in part by the European Research Council under the Horizon 2020 Programme, ERC Grant Agreement No. 740269. MEC is funded by the Royal Society.

\* [tb698@cam.ac.uk](mailto:tb698@cam.ac.uk)

- [1] L. D. Landau and E. M. Lifshitz, *Statistical Physics, Course on Theoretical Physics, Vol. 5*, Pergamon Press, Oxford (1970).
- [2] J. P. Bouchaud, *J. Phys. I (France)* **2**, 1705 (1992).
- [3] G. Bel and E. Barkai, *Phys. Rev. Lett.* **94**, 240602 (2005).
- [4] G. M. Schütz and S. Trimper, *Phys. Rev. E* **70**, 045101(R) (2004).
- [5] A. A. Budini, *Phys. Rev. E* **94** 022108 (2016).
- [6] R.G. Palmer, *Advances in Physics* **31**, 669 (1982).
- [7] N. Goldenfeld, *Lectures on Phase transitions and the Renormalization Group* (Frontiers in Physics-85), CRC Press, Boca Raton, Florida, 2018.
- [8] E. Fermi, J. Pasta and S. Ulam, Los Alamos Report LA-1940 (1955).
- [9] G. P. Berman and F. M. Izrailev, *Chaos* **15**, 015104 (2005).
- [10] B. Derrida and A. Gerschenfeld, *J. Stat. Phys.* **137**, 978 (2009).
- [11] A. G. Cherstvy, A. V. Chechkin and R. Metzler, *New Journal of Physics* **15**, 083039 (2013).
- [12] T. Banerjee, S. N. Majumdar, A. Rosso and G. Schéhr, *Phys. Rev. E* **101**, 052101 (2020).
- [13] H. van Beijeren, *J. Stat. Phys.* **63**, 47 (1991).
- [14] N. Leibovich and E. Barkai, *Phys. Rev. E* **88** 032107 (2013).
- [15] P. L. Krapivsky, K. Mallick and T. Sadhu, *Phys. Rev. Lett.* **113**, 078101 (2014).
- [16] J. Cividini and A. Kundu, *J. Stat. Mech.* 083203 (2017).
- [17] J. Rana and T. Sadhu, *arxiv:2203.01609* (2022).
- [18] S. Kwon and J. M. Kim, *Phys. Rev. E* **96** 012146 (2017).
- [19] K. Binder and A. P. Young, *Rev. Mod. Phys.* **58**, 801 (1986).
- [20] R. Dreyfus, Y. Xu, T. Still, L. A. Hough, A. G. Yodh, and S. Torquato, *Phys. Rev. E* **91**, 012302 (2015).
- [21] Ü Seleme Nizam *et al*, *J. Phys.: Condens. Matter* **33** 304002 (2021).
- [22] S. F. Knowles, N. E. Weckman, V. J. Y. Lim, D. J. Bonthuis, U. F. Keyser, and A. L. Thorneywork, *Phys. Rev. Lett.* **127**, 137801 (2021).
- [23] P. M. Chaikin and T. C. Lubensky, *Principles of Condensed Matter Physics*, Cambridge University Press, Cambridge (2013).
- [24] J. S. Bell, *Phys. Rev.* **129**, 1896 (1963).
- [25] U. Fano, *Phys. Rev.* **72**, 26 (1947).
- [26] S. Torquato, *Physics Reports* **745**, 1 (2018).
- [27] A. L. Hodgkin and R. D. Keynes, *J. Physiol.* **128** 61 (1955).
- [28] T. E. Harris, *J. Appl. Probab.* **2**, 323 (1965).
- [29] P. M. Richards, *Phys. Rev. B* **16**, 1393 (1977).
- [30] S. Alexander and P. Pincus, *Phys. Rev. B* **18** 2011 (1978).
- [31] R. Arratia, *Ann. Probab.* **11**, 362 (1983).
- [32] C. Hegde, S. Sabhapandit and A. Dhar, *Phys. Rev. Lett.* **113**, 120601 (2014).
- [33] Q-H. Wei, C. Bechinger and P. Leiderer, *Science* **287**, 625 (2000).
- [34] L. Bertini, A. De Sole, D. Gabrielli, G. Jona-Lasinio and C. Landim, *Rev. Mod. Phys.* **87**, 593 (2015).
- [35] B. Derrida, *J. Stat. Mech.* (2011) P01030; B. Derrida, *J. Stat. Mech.* (2007) P07023.
- [36] T. Bodineau and B. Derrida, *Phys. Rev. Lett.* **92**, 180601

- (2004).
- [37] L. Bertini, A. De Sole, D. Gabrielli, G. Jona-Lasinio and C. Landim, Phys. Rev. Lett. **87**, 040601 (2001).
- [38] G. Jona-Lasinio, J. Stat. Mech., P02004 (2014).
- [39] T. Imamura, K. Mallick and T. Sasamoto, Phys. Rev. Lett. **118**, 160601 (2017)
- [40] K. Mallick, H. Moriya and T. Sasamoto, arxiv:2202.05213 (2022).
- [41] M. Kollmann, Phys. Rev. Lett. **90**, 180602 (2003).
- [42] L. Lizana, T. Ambjörnsson, A. Taloni, E. Barkai and M. A. Lomholt, Phys. Rev. E **81**, 051118 (2010).
- [43] A. Poncet, A. Grabsch, P. Illien, O. Bénichou, Phys. Rev. Lett. **127**, 220601 (2021).
- [44] A. Grabsch, A. Poncet, P. Rizkallah, P. Illien and O. Bénichou, Science Advances **8**, eabm5043 (2022).
- [45] R. Rajesh and S. N. Majumdar, Phys. Rev. E **64**, 036103 (2001).
- [46] see the Supplemental Material.
- [47] I. Santra, U. Basu, S. Sabhapandit, arXiv preprint arXiv:2202.12117 (2022).
- [48] M. Bothe and G. Pruessner, Phys. Rev. E **103**, 062105 (2021).
- [49] D. Martin, J. O’Byrne, M. E. Cates, É. Fodor, C. Nardini, J. Tailleur, and F. van Wijland, Phys. Rev. E **103** 032607 (2021).
- [50] C. Bechinger, R. Di Leonardo, H. Löwen, C. Reichhardt, G. Volpe, and G. Volpe, Rev. Mod. Phys. **88**, 045006 (2016).
- [51] U. Basu, S. N. Majumdar, A. Rosso and G. Schehr, Phys. Rev. E **98**, 062121 (2018).
- [52] K. Malakar *et al*, J. Stat. Mech. (2018) 043215 .
- [53] T. Demaerel and C. Maes, Phys. Rev. E **97**, 032604 (2018).
- [54] M. E. Cates and J. Tailleur, Europhys. Lett. **101**, 20010 (2013).
- [55] T. Banerjee, R. L. Jack and M. E. Cates, J. Stat. Mech **2022**, 013209 .
- [56] S. N. Majumdar and M. Barma, Phys. Rev. B **44**, 5306 (1991).
- [57] E. Barkai and R. Silbey, Phys. Rev. Lett. **102**, 050602 (2009).
- [58] A. De Masi and P. A. Ferrari, J. Stat. Phys. **38**, 603 (1985).
- [59] E Mallmin, R. A. Blythe and M. R. Evans, J. Stat. Mech. (2021) 013209.
- [60] T-H Liu and C. C. Chang, Nanoscale, **7**, 10648 (2015).
- [61] M. M. R. Williams, Math. Proc: Camb. Phil. Soc., **84**, 549 (1978).
- [62] R. Villavicencio-Sanchez, R. J. Harris and H. Touchette, EPL, **105** 30009 (2014).

# Supplemental Material for “Role of initial conditions in 1D diffusive systems: compressibility, hyperuniformity and long-term memory”

Tirthankar Banerjee,<sup>1,\*</sup> Robert L. Jack,<sup>1,2</sup> and Michael E. Cates<sup>1,†</sup>

<sup>1</sup>*DAMTP, Centre for Mathematical Sciences, University of Cambridge, Wilberforce Road, Cambridge, CB3 0WA*

<sup>2</sup>*Yusuf Hamied Department of Chemistry, University of Cambridge, Lensfield Road, Cambridge CB2 1EW, United Kingdom*

In the following we present some supplemental information, to provide additional detail on the discussion of the main text. In Sec. I we describe a set of translationally invariant initial states with Fano factor  $\alpha_{ic} \leq 1$ , which are used as initial conditions for the numerical computations in the main text. Section II contains additional details of the numerical results. In Sec. III, we give a full derivation of the tracer variance for systems described by Macroscopic Fluctuation Theory. This computation is included for completeness, it largely follows Ref [1], with some modifications to account for the general class of initial conditions considered in this work.

## I. MICROSCOPIC EXAMPLE FOR THE FANO FACTOR $\alpha_{ic}$ : HARD RODS IN ONE DIMENSION

### A. Theory

A central role in this work is played by the Fano factor  $\alpha_{ic}$ . As an example of an equilibrium system where this quantity can be varied continuously between 0 and 1, we consider hard particles of size  $r_0$ , in one dimension. For any configuration of  $N$  such particles in a box of size  $L$ , there is a corresponding configuration of point particles in a box of size  $L - Nr_0$ . The two configurations are related by ordering the positions of the point particles as  $\tilde{x}_1, \tilde{x}_2, \dots, \tilde{x}_N$ , and then defining the positions of the hard particles as  $x_m = \tilde{x}_m + (m - 1)r_0$ . Clearly  $r_0 \leq L/N$  in order that the hard particles can fit inside the box.

Since this transformation has unit Jacobian, the configurational partition function for the hard rods is the same as that of the point particles, that is

$$\mathcal{Z} = \frac{(L - Nr_0)^N}{N!}. \quad (S1)$$

and the corresponding pressure  $P$  is given by

$$\beta P = \frac{\partial}{\partial L}(\ln \mathcal{Z}) = \frac{N}{L - Nr_0}, \quad (S2)$$

where  $\beta$  is the inverse temperature (divided by Boltzmann’s constant).

Recall that the (mean) density is  $\bar{\rho} = N/L$ . Observe that  $0 \leq \bar{\rho}r_0 \leq 1$ , where the lower limit corresponds to point particles (hard rods of size zero) and the upper limit to the case where the hard rods fill the box exactly. It is convenient to define a dimensionless quantity:

$$\zeta = \frac{L - Nr_0}{Nr_0} = \frac{1 - \bar{\rho}r_0}{\bar{\rho}r_0}, \quad (S3)$$

which diverges for point particles, and approaches zero for the case where the rods fill the box.

From (S2), we can calculate the (isothermal) compressibility  $\kappa$  as

$$\kappa = -\frac{1}{L} \frac{\partial L}{\partial P} = \frac{\beta(1 - \bar{\rho}r_0)^2}{\bar{\rho}}. \quad (S4)$$

Then it is well-known (by considering large systems in the grand canonical ensemble [2, 3]) that the Fano factor for fluctuations of the particle number is

$$\alpha_{ic} = \frac{\text{Var}(n)}{\langle n \rangle} = \frac{\kappa \bar{\rho}}{\beta} \quad (S5)$$

\*Electronic address: tb698@cam.ac.uk

†Electronic address: m.e.cates@damtp.cam.ac.uk

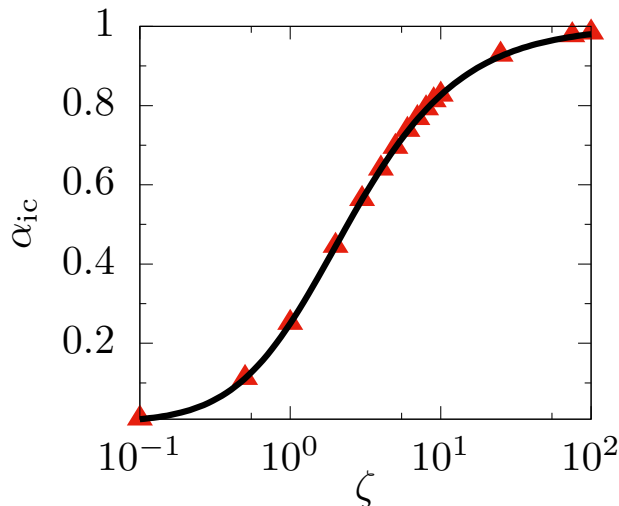


FIG. S1: Numerically estimated  $\alpha_{ic}$  from hard rod configurations with varying  $\zeta$ . The line shows the prediction (S6). Results were obtained at density  $\bar{\rho} = 1$  in a system of  $N = 10000$  particles.

(The result for  $\alpha_{ic}$  is the same if one considers a large grand-canonical system, or a large subsystem of size  $\ell$  in a very large canonical system.) For the present system (S3) and (S4) yield

$$\alpha_{ic} = \left( \frac{\zeta}{1 + \zeta} \right)^2. \quad (\text{S6})$$

Since  $0 \leq \zeta < \infty$ , one sees that these states have  $0 \leq \alpha_{ic} \leq 1$ .

### B. Numerical generation of states with prescribed $\alpha_{ic}$

The above analysis provides a method for generating states with prescribed  $\alpha_{ic}$ . This method was used in the simulations described in the main text. Specifically: for any  $\bar{\rho}, \alpha_{ic}$ , Eqs. (S3,S6) can be solved for the corresponding  $r_0$ . Then, for initial states with all particles to the left of the origin (as required for numerical computations of the  $Q(T)$ ), we start by placing  $N$  point particles at random between  $-L$  and  $-Nr_0$ . Similar to the construction above, these positions can be ordered in an increasing sequence as  $\tilde{x}_1, \dots, \tilde{x}_N$  and the position of the  $m$ th hard particle is obtained as  $x_m = \tilde{x}_m + (m - 1)r_0$ .

For initial states with particles on both sides of the origin (as required for simulations of tracer motion), we start with the same method identified above. Then we identify the central particle as the tracer, and we shift the whole configuration so that the tracer starts at the origin.

To confirm that these methods work as expected, we generated configurations in this way. Measuring the asymptotic variance  $\alpha_{ic}$  numerically requires some care because the number of particles is finite in the simulations, which are performed in the canonical ensemble. Let  $n(\ell)$  denote the number of particles within a distance  $\ell$  of the origin. We measured the mean and variance of this number, as a function of  $\ell$ . By homogeneity,  $\langle n(\ell) \rangle = \bar{\rho}\ell$ . Also, the variance is found to be  $\text{Var}[n(\ell)] \simeq \alpha\ell(L - \ell)N/L^2$  [valid for large  $N, L$  with  $N/L = \bar{\rho}$  and  $\ell \gg 1$ ].

Note in particular  $\text{Var}[n(L)] = 0$  because the total number of particles is fixed. To obtain  $\alpha_{ic}$ , we note that its definition includes a limit of large  $\ell$ , which must be taken *after* the thermodynamic limit  $L \rightarrow \infty$  (at fixed  $\bar{\rho}$ ). That is

$$\alpha_{ic} = \lim_{\ell \rightarrow \infty} \lim_{L \rightarrow \infty} \frac{\text{Var}[n(\ell)]}{\langle n(\ell) \rangle} = \alpha$$

Since  $\ell \ll L$ , this result is independent of the ensemble. In practice we take configurations from the canonical ensembles as above (fixed  $N$ ) and we fit numerical data for  $\text{Var}[n(\ell)]$  to the quadratic form  $\alpha\bar{\rho}\ell(L - \ell)/L$  in order to obtain  $\alpha$  as an estimate of  $\alpha_{ic}$ . We show in Fig. S1 that the results agree perfectly with the prediction (S6).

Note that states with  $\alpha_{ic} > 1$  can be generated in principle, by first distributing all point particles on the line uniformly for a given  $\bar{\rho}$ , adding suitable local attractive interactions between particles, and equilibrating the system. We do not consider such states in our numerical computations.



## II. NUMERICAL SCHEMES : FURTHER DETAILS

We briefly describe additional numerical schemes used to obtain the numerical results in the main text (Figs. 1 and 2) .

### A. Hyperuniform initial states

For hard-rod configurations, there is a hyperuniform (HU) state where  $L = Nr_0$ , so all particles are touching their neighbours. The particles are equispaced, the system resembles a crystal, and  $\alpha_{ic} = 0$ . As described in the main text, results that depend only on  $\alpha_{ic}$  must give the same result for any HU initial condition.

To test this, we modify these equispaced configurations by short-ranged perturbations, which do not disturb the long wavelength density fluctuations, and hence preserve the HU property. Specifically, we add independent and identically distributed random increments to each particle position: the increment is  $\pm\delta$  where positive and negative signs are each chosen with probability 1/2. (For the case where all particles are initialised to the left of the origin, particles within  $\delta$  of the origin are we always incremented by  $-\delta$ .) For the ‘‘randomized HU’’ initial conditions with  $\alpha_{ic} = 0$  shown in Fig. 1(a) of the main text, the density is  $\bar{\rho} = 1$  and we take  $\delta = 5$ , so particles are displaced by several times their typical spacing. For Fig. 2(b) we have similarly  $\bar{\rho} = 10$  and  $\delta = 1$ .

### B. Dynamics

For the non-interacting problem we study four different models, all of which have late-time Gaussian statistics. We list these in the following:

*Passive Brownian motion:* Particle  $i$  undergoes Brownian motion according to

$$\dot{x}_i = \sqrt{2D}\eta_i(t), \quad (S7)$$

where  $D$  is the diffusivity, and  $\eta_i(t)$  is a zero-mean white noise with a variance,  $\langle \eta_i(t)\eta_j(t') \rangle = \delta(t-t')\delta_{ij}$ . The variance of the current associated with this system of particles, starting from a step-like initial set-up and different values of  $\alpha_{ic}$  is plotted in Fig.1(a) of the main text. We took  $\bar{\rho} = 1$  and  $D = 1$ , with  $N = 4000$ . The data was averaged over  $10^6$  realizations.

*Run and tumble particles:* The dynamics of each run-and-tumble particle (RTP)  $i$  is given by [4, 5]:

$$\dot{x}_i = v\sigma_i(t), \quad (S8)$$

where  $v$  is the velocity and  $\sigma_i(t)$  is a noise that flips at a Poisson rate  $\gamma$  between two values  $\pm 1$ . It is well known [4] that the late-time behaviour ( $t \gg \gamma^{-1}$ ) of such particles is Gaussian, with an effective diffusivity  $D = \frac{v^2}{2\gamma}$ . In Fig.1(b), the temporal evolution of  $\text{Var}[Q(T)]$  for RTPs is shown by squares. We choose  $v = 1, \gamma = 0.5, \bar{\rho} = 1, N = 1000$ . The data was averaged over  $\sim 10^5$  samples.

*Active Ornstein-Uhlenbeck particles:* The equations of motion for an active Ornstein-Uhlenbeck particle (AOUP), without any external or interaction potential, are given by [6] :

$$\begin{aligned} \dot{x}_i &= v_i + \sqrt{2D_x}\eta_i^x(t) \\ \tau\dot{v}_i &= -v_i + \sqrt{2D_v}\eta_i^v(t), \end{aligned} \quad (S9)$$

where  $x_i$  and  $v_i$ , respectively are the position and propulsive velocity of particle  $i$ , and the  $\eta_i^a(t)$  are zero-mean Gaussian white noises with variances  $\langle \eta_i^a(t)\eta_j^b(t') \rangle = \delta(t-t')\delta_{ij}\delta_{ab}$ , with  $a, b = x, v$ . Also,  $D_x$  and  $D_v$  are the noise strengths associated with  $\eta_i^x(t)$  and  $\eta_i^v(t)$ , respectively. For  $\tau = 0$ , we have simple passive Brownian motion, with effective diffusivity  $D = D_v + D_x$ . A finite  $\tau$  acts as a characteristic persistence time, thus (only) lending inertia to the particle motion. For  $t \gg \tau$ , each AOUP behaves diffusively, following  $D = D_v + D_x$ . In Fig.1(b) of the main text, we use  $v_0 = 0, D_x = 0.5 = D_v, \tau = 1, \bar{\rho} = 1$  and  $N = 1000$ . Results of  $\text{Var}[Q(T)]$  for AOUPs (averaged over  $\sim 10^5$  samples) are shown by circles in Fig.1(b).

*Active Brownian particles:* The Langevin equations of motion for a free active Brownian particle (ABP)  $i$  in one dimension can be written as [7, 8]

$$\begin{aligned}\dot{x}_i &= v \cos \theta_i \\ \dot{\theta}_i &= 2D_R \eta_i(t),\end{aligned}\tag{S10}$$

where  $x_i$  gives the instantaneous position of the particle,  $\theta_i$  represents the particle orientation that itself follows diffusive dynamics with a rotational diffusion constant  $D_R$ .  $\eta_i(t)$  is a delta-correlated, zero mean Gaussian white noise. Free AOUPs behave diffusively with effective diffusivity  $D = \frac{v^2}{2D_R}$  for times  $t \gg D_R^{-1}$  [7]. In Fig1(b) of the main text, we use  $v = 1, D_R = 0.5$  for each ABP. The initial orientation for each particle is chosen randomly between 0 and  $2\pi$ . We choose  $\bar{\rho} = 1, N = 1000$ . The results for  $\text{Var}[Q(T)]$  (averaged over  $\sim 10^5$  samples) are represented by triangles in Fig.1(b).

*Interacting hardcore Brownian particles:* Here we use  $N = 10000 + 1$  particles located within  $-L/2$  and  $L/2$ , with  $\bar{\rho} = 10$  and the tracer located centrally at the origin. We follow the technique of [9]. We let the particles evolve independently up to time  $T$ , and note the position of the new central particle, which equivalently gives the displacement of the tracer in a system of hard Brownian particles. The data was averaged over  $\sim 10^5$  realizations.

### III. MACROSCOPIC FLUCTUATION THEORY FOR THE INITIAL STATE WITH ARBITRARY $\alpha_{ic}$

We present a systematic derivation to show that the Fano factor  $\alpha_{ic}$  of the initial state determines the variance of tracer position  $X(T)$  at some late-time  $T$ , for a general class of interacting particles whose dynamics is described by the framework of Macroscopic Fluctuation Theory (MFT). We follow exactly the procedure introduced in [1], where the analysis is set up first as a large deviation problem through the optimal solutions of the action, and then the variance  $\text{Var}[X(T)]$  of the tracer position is extracted by a perturbative expansion in orders of  $\lambda$ , which is the Laplace variable corresponding to  $X(T)$  in its cumulant generating function. It is essential that particles undergo single-file motion, in particular, the tracer cannot pass its neighbours. We also assume that the tracer starts from the origin, so  $X(T)$  can be interpreted either as its position, or its displacement.

Within the MFT framework, the evolution of the macroscopic density  $\rho(x, t)$  is given by [10, 11]

$$\partial_t \rho(x, t) = \partial_x [D(\rho) \partial_x \rho(x, t) + \sqrt{\sigma(\rho)} \eta(x, t)],\tag{S11}$$

where  $\sigma(\rho)$  and  $D(\rho)$  are the mobility and diffusivity, respectively, while  $\eta(x, t)$  is a Gaussian white noise with zero mean and a variance  $\langle \eta(x, t) \eta(x', t') \rangle = \delta(x - x') \delta(t - t')$ .

Let  $X(T)$  be the position of the tracer particle at the final (observation) time  $T$ . Due to the single-file constraint, this position can be expressed as a functional of the density  $\rho(x, t)$ . To see this, note that the numbers of particles to left and right of the tracer must both remain constant. At time  $t$ , the number of particles to the right of the tracer is  $\int_{X(t)}^{\infty} \rho(x, t) dx$ : this must be equal at times  $t = 0, T$ , which yields

$$\int_0^{X(T)} dx \rho(x, T) = \int_0^{\infty} dx [\rho(x, T) - \rho(x, 0)].\tag{S12}$$

(we used that  $X_0 = 0$ ). This formula allows the tracer position to be expressed as a functional of the density field  $X(T) = X[\rho(x, T)]$ .

The statistics of  $X(T)$  can be extracted from the moment generating function  $\langle e^{\lambda X(T)} \rangle$ , which can be expressed as a path integral in the Martin-Siggia-Rose formalism [1]

$$\langle e^{\lambda X(T)} \rangle = \int \mathcal{D}[\rho(x, t), \hat{\rho}(x, t)] e^{-\mathcal{S}[\rho(x, t), \hat{\rho}(x, t)]},\tag{S13}$$

where  $\hat{\rho}(x, t)$  is a response field, and the action  $\mathcal{S}[\rho(x, t), \hat{\rho}(x, t)]$  is given by

$$\mathcal{S}[\rho(x, t), \hat{\rho}(x, t)] = -\lambda X(T)[\rho] + F[\rho(x, 0)] + \int_0^T dt \int_{-\infty}^{\infty} dx \left\{ \hat{\rho} \partial_t \rho - \frac{\sigma(\rho)}{2} (\partial_x \hat{\rho})^2 + D(\rho) (\partial_x \rho) (\partial_x \hat{\rho}) \right\}.\tag{S14}$$

where  $F[\rho(x, 0)] = -\ln(\text{Prob}[\rho(x, 0)])$  captures the information about the initial state, with  $\text{Prob}[\rho(x, 0)]$  being the probability of observing an initial density profile  $\rho(x, 0)$ .

### A. Initial conditions and the functional $F$

So far the analysis follows [1]. However, the present derivation requires a more detailed treatment of the functional  $F$ , as we now discuss. We first discuss this functional in the case where the initial condition is an equilibrium state with free energy density  $f_{\text{ic}}(\rho)$ : we explain below how the analysis is generalised to cover non-equilibrium initial states. Note: this  $f_{\text{ic}}$  differs in general from the free energy  $f_{\text{eq}}$  associated with the equilibrium state of the model dynamics, which obeys the fluctuation-dissipation theorem  $f_{\text{eq}}''(\rho) = 2D(\rho)/\sigma(\rho)$  [10]. Taking  $f_{\text{ic}} = f_{\text{eq}}$  will recover the annealed result of [1], but the following analysis is more general, in that it applies for a general  $f_{\text{ic}}$ , corresponding to initial conditions that are not sampled from the equilibrium stationary state of the underlying model.

For an initial condition taken from the equilibrium state with free energy  $f_{\text{ic}}$ , the hydrodynamic density fluctuations behave (on large length scales) as

$$-\ln \text{Prob}[\rho] = F[\rho] \simeq \int_{-\infty}^{\infty} dx g_{\text{ic}}(\rho) \quad (\text{S15})$$

with

$$g_{\text{ic}}(\rho) = f_{\text{ic}}(\rho) - f_{\text{ic}}(\bar{\rho}) - (\rho - \bar{\rho})f_{\text{ic}}'(\bar{\rho}) \quad (\text{S16})$$

as given in Eq. (5.1) of [10]. The most probable initial condition is  $\rho(x, 0) = \bar{\rho}$ , which has  $F = 0$ . Write

$$\begin{aligned} f_{\text{ic}}(\rho) - f_{\text{ic}}(\bar{\rho}) - (\rho - \bar{\rho})f_{\text{ic}}'(\bar{\rho}) &= \int_{\bar{\rho}}^{\rho} dr [f_{\text{ic}}'(r) - f_{\text{ic}}'(\bar{\rho})] \\ &= \int_{\bar{\rho}}^{\rho} dr f_{\text{ic}}''(r) [\rho - r] \end{aligned} \quad (\text{S17})$$

where the second equality uses an integration by parts. Hence

$$F[\rho(x, 0)] = \int_{-\infty}^{\infty} dx \int_{\bar{\rho}}^{\rho(x, 0)} dr g_{\text{ic}}''(r) [\rho(x, 0) - r], \quad (\text{S18})$$

where we used  $f_{\text{ic}}''(\rho) = g_{\text{ic}}''(\rho)$ . To capture the typical fluctuations of  $\rho$ , it is sufficient to expand  $F$  to quadratic order, yielding

$$F[\rho(x, 0)] \approx \frac{1}{2} \int_{-\infty}^{\infty} dx g_{\text{ic}}''(\bar{\rho}) [\rho(x, 0) - \bar{\rho}]^2 \quad (\text{S19})$$

At this order, recall that  $F$  is the log-probability associated with density fluctuations in the initial state, and note that  $n(\ell) = \int_0^{\ell} \rho(x, 0) dx$  is Gaussian with mean  $\ell\bar{\rho}$  and variance  $\ell/g_{\text{ic}}''(\bar{\rho})$ , hence the Fano factor for the initial condition is

$$\alpha_{\text{ic}} = \frac{1}{\bar{\rho} g_{\text{ic}}''(\bar{\rho})}. \quad (\text{S20})$$

To understand the role of initial states that are not equilibrium states, we note that the only assumption required in the following is that fluctuations have log-probability (S19), where  $g_{\text{ic}}''(\bar{\rho})$  is some positive constant. This result is assumed to hold on large (hydrodynamic) scales, so it is natural that the integrand is local. In other words, we require that the hydrodynamic density has Gaussian statistics, without any long-ranged interactions. In this case the asymptotic variance  $\alpha_{\text{ic}}$  is necessarily related to  $f_{\text{ic}}''$  by (S20) and we arrive at

$$F[\rho(x, 0)] \approx \frac{1}{2} \int_{-\infty}^{\infty} \frac{dx}{\bar{\rho} \alpha_{\text{ic}}} [\rho(x, 0) - \bar{\rho}]^2, \quad (\text{S21})$$

which will be assumed to hold at quadratic order in  $\rho - \bar{\rho}$ : this is consistent with the form of  $g_{\text{ic}}$  in (19) of the main text.

### B. Path of least action

As anticipated above, the strategy for computing  $\text{Var}[X(T)]$  is to consider large deviations of  $X(T)$  as  $T \rightarrow \infty$ , but working to quadratic order in the size of these deviations. We follow [1], with suitable modifications to allow for a

flexible choice of initial condition. We write the cumulant generating function for  $X(T)$  as  $\mu(\lambda) = \ln\langle e^{\lambda X(T)} \rangle$ . This can be estimated from (S13) using a saddle point method:

$$\mu(\lambda) = -\mathcal{S}[q(x, t), p(x, t)] \quad (\text{S22})$$

where  $[\rho, \hat{\rho}] = [q, p]$  is the path that minimises the action  $\mathcal{S}$ . Note that  $\text{Var}[X(T)] = \mu''(0)$  so it will be sufficient in the following to work to quadratic order in  $\lambda$ . To find the path of least action, expand  $\mathcal{S}$  about  $(q, p)$  and set the first variation to zero: one obtains Euler-Lagrange equations

$$\begin{aligned} \partial_t q - \partial_x(D(q)\partial_x q) &= -\partial_x(\sigma(q)\partial_x p) \\ \partial_t p + D(q)\partial_{xx} p &= -\frac{1}{2}\sigma'(q)(\partial_x p)^2. \end{aligned} \quad (\text{S23})$$

The action is minimised at fixed  $\lambda$  so the final position of the tracer  $X(T)$  is also a variable to be optimised: denote the optimal value of this variable by  $Y(T)$ . The boundary condition for  $t = T$  is obtained by extremising the action with respect to  $\rho(x, T)$  and using (S12) [1]:

$$p(x, T) = \frac{\lambda}{q(Y, T)} \Theta(x - Y). \quad (\text{S24})$$

where  $\Theta(x)$  is the Heaviside function. The boundary condition at time  $t = 0$  is obtained similarly by extremising the action with respect to  $\rho(x, 0)$

$$p(x, 0) = \frac{\lambda}{q(Y, T)} \Theta(x) + \frac{\delta}{\delta q(x, 0)} F[q(x, 0)]. \quad (\text{S25})$$

Using results obtained so far, (S22) becomes

$$\mu(\lambda) = \lambda Y - F[q(x, 0)] - \int_0^T dt \int_{-\infty}^{\infty} dx \frac{\sigma(q(x, T))}{2} (\partial_x p(x, t))^2. \quad (\text{S26})$$

As noted above, we are only interested in the variance of  $X(T)$ , so it is sufficient to make a perturbative expansion in  $\lambda$  for  $q(x, t)$ ,  $p(x, t)$ , and  $Y(T)$ . We work at quadratic order in  $\lambda$ . For  $\lambda = 0$  the path of least action corresponds to the typical behaviour of the system, which is a homogeneous state  $q(x, t) = \bar{\rho}$  with typical noise realisations  $p(x, t) = 0$ , and no net tracer motion in either direction  $Y(T) = 0$ . To leading order in  $\lambda$ , we have therefore

$$q(x, t) = \bar{\rho} + \lambda q_1(x, t) + \dots \quad (\text{S27})$$

$$p(x, t) = \lambda p_1(x, t) + \dots \quad (\text{S28})$$

$$Y(T) = \lambda Y_1 + \dots \quad (\text{S29})$$

Expanding (S26) in  $\lambda$ , the first terms appear at quadratic order, yielding

$$\frac{1}{2} \text{Var}[X(T)] = Y_1 - \frac{1}{2} \int_{-\infty}^{\infty} dx \frac{q_1(x, 0)^2}{\bar{\rho}\alpha_{ic}} - \frac{\sigma(\bar{\rho})}{2} \int_0^T dt \int_{-\infty}^{\infty} dx (\partial_x p_1(x, t))^2. \quad (\text{S30})$$

where we used (S21).

At leading order in  $\lambda$ , (S12) becomes

$$\int_0^{\lambda Y_1} \bar{\rho} dx = \int_0^{\infty} dx [\lambda q_1(x, T) - \lambda q_1(x, 0)], \quad (\text{S31})$$

which allows the tracer displacement to be expressed in terms of the density field as

$$Y_1 = \frac{1}{\bar{\rho}} \int_0^{\infty} dx [q_1(x, T) - q_1(x, 0)]. \quad (\text{S32})$$

Also, substituting (S27) and (S28) in (S23), we obtain the Euler-Lagrange equations to first order in  $\lambda$ :

$$\partial_t q_1(x, t) - D(\bar{\rho})\partial_{xx} q_1(x, t) = -\sigma(\bar{\rho}) \partial_{xx} p_1(x, t). \quad (\text{S33})$$

$$\partial_t p_1(x, t) + D(\bar{\rho})\partial_{xx} p_1(x, t) = 0 \quad (\text{S34})$$

The boundary condition (S24) at leading order in  $\lambda$  becomes

$$p_1(x, T) = \Theta(x)/\bar{\rho} \quad (\text{S35})$$

The equations for  $p_1$  are now closed, and can be solved as

$$p_1(x, t) = \frac{1}{2\bar{\rho}} \operatorname{erfc} \left( \frac{-x}{\sqrt{4D(\bar{\rho})(T-t)}} \right). \quad (\text{S36})$$

For the boundary condition (S25), use (S21) to obtain  $\delta F/\delta q \approx \lambda q_1/(\bar{\rho}\alpha_{\text{ic}})$  and hence

$$\begin{aligned} q_1(x, 0) &= \alpha_{\text{ic}}\bar{\rho}[p_1(x, 0) - \Theta(x)/\bar{\rho}] \\ &= \alpha_{\text{ic}}\bar{\rho}[p_1(x, 0) - p_1(x, T)]. \end{aligned} \quad (\text{S37})$$

where the second equality used (S35). (This is one point where the general initial condition enters, and the computation differs from [1].)

Hence we have derived the equations for the instanton, corresponding to (20-22) of the main text. As described in the main text, this allows the initial condition of the least-action path to be identified, corresponding to an imbalance of density to the left and right of the tracer.

### C. Tracer variance for HU initial condition

For the HU initial condition ( $\alpha_{\text{ic}} = 0$ ), the variance of  $X(T)$  can now be computed, again following [1]. Plugging (S32) and (S37) into (S30) and setting  $\alpha_{\text{ic}} = 0$  yields

$$\Delta X_{\text{noise}}^2(T) = \operatorname{Var}[X(T)] = \frac{2}{\bar{\rho}} \int_0^\infty dx q_1(x, T) - \sigma(\bar{\rho}) \int_0^T dt \int_{-\infty}^\infty dx (\partial_x p_1(x, t))^2 \quad (\text{S38})$$

where we have identified  $\Delta X_{\text{noise}}^2(T)$  with the tracer variance computed at  $\alpha_{\text{ic}} = 0$ . Expressing  $q_1(x, t)$  as a product of forward and backward diffusion propagators, followed by some algebra [1], one finds

$$\Delta X_{\text{noise}}^2(T) = \frac{\sigma(\bar{\rho})}{\bar{\rho}^2} \sqrt{\frac{T}{2\pi D(\bar{\rho})}}. \quad (\text{S39})$$

This result is quoted in (24) of the main text. This computation shows that any HU initial state (i.e., including states with short-ranged and finite density correlations) will lead to (S39), and that this result is not restricted to the quenched case considered in [1] (where the initial state has no density fluctuations at all).

### D. Tracer variance for general initial condition

We now calculate  $\operatorname{Var}[X(T)]$  for  $\alpha_{\text{ic}} > 0$ . Noting the linearity of (S33), the least-action path  $q_1(x, t)$  can be divided into two contributions, similar to [1]:

$$q_1(x, t) = q_{\text{I}}(x, t) + q_{\text{h}}(x, t), \quad (\text{S40})$$

where  $q_{\text{h}}(x, t)$  represents the solution of the homogeneous equation

$$\partial_t q_{\text{h}}(x, t) - D(\bar{\rho})\partial_{xx} q_{\text{h}}(x, t) = 0, \quad (\text{S41})$$

with the inhomogeneous boundary condition

$$q_{\text{h}}(x, 0) = \alpha_{\text{ic}}\bar{\rho}[p_1(x, 0) - p_1(x, T)], \quad (\text{S42})$$

while  $q_{\text{I}}$  satisfies the inhomogeneous equation

$$\partial_t q_{\text{I}}(x, t) - D(\bar{\rho})\partial_{xx} q_{\text{I}}(x, t) = -\sigma(\bar{\rho})\partial_{xx} p_1(x, t), \quad (\text{S43})$$

with homogeneous boundary condition  $q_I(x, 0) = 0$ .

Comparing with the case  $\alpha_{ic} = 0$  considered above, observe that  $q_I(x, t)$  is the same least-action path as we already considered, for the HU initial condition. Noting that the solution (S36) for  $p_1$  is independent of  $\alpha_{ic}$ , and that  $q_I(x, 0) = 0$ , Eq. (S30) becomes

$$\text{Var}[X(T)] - \Delta X_{\text{noise}}^2(T) = \frac{2}{\bar{\rho}} \int_0^\infty dx [q_h(x, T) - q_h(x, 0)] - \frac{1}{\bar{\rho}\alpha_{ic}} \int_{-\infty}^\infty dx (q_h(x, 0))^2 \quad (\text{S44})$$

It only remains to compute the right hand side of (S44), as in [1]. To obtain a preliminary result, combine (S34) and (S41) to obtain

$$\partial_t [p_1(x, t)q_h(x, t)] = -D(\bar{\rho}) \partial_x [q_h(x, t)\partial_x p_1(x, t) - p_1(x, t)\partial_x q_h(x, t)]. \quad (\text{S45})$$

This is a continuity equation for  $p_1 q_h$ , so the integral of that quantity is conserved:

$$\frac{\partial}{\partial t} \int_{-\infty}^\infty dx p_1(x, t)q_h(x, t) = 0. \quad (\text{S46})$$

Now write  $I = \int_0^\infty dx [q_h(x, T) - q_h(x, 0)]/\bar{\rho}$  for the first term on the right hand side of (S44). Then

$$\begin{aligned} I &= \int_{-\infty}^\infty dx \frac{\Theta(x)}{\bar{\rho}} [q_h(x, T) - q_h(x, 0)] \\ &= \int_{-\infty}^\infty dx p_1(x, T)q_h(x, T) - \int_{-\infty}^\infty dx p_1(x, T)q_h(x, 0) \\ &= \int_{-\infty}^\infty dx p_1(x, 0)q_h(x, 0) - \int_{-\infty}^\infty dx p_1(x, T)q_h(x, 0), \end{aligned} \quad (\text{S47})$$

where the second step uses (S35), and the final step uses (S46). Combining the integrals and using (S42) to substitute for  $p_1(x, T) - p_1(x, 0)$ , we obtain

$$I = \frac{1}{\bar{\rho}\alpha_{ic}} \int_{-\infty}^\infty dx (q_h(x, 0))^2. \quad (\text{S48})$$

Hence the right hand side of (S44) can be simplified as  $2I - I = I$ , and using (S42,S36) yields

$$\text{Var}[X(T)] - \Delta X_{\text{noise}}^2(T) = \alpha_{ic}\bar{\rho} \int_{-\infty}^\infty dx \left[ \frac{\Theta(x)}{\bar{\rho}} - \frac{1}{2\bar{\rho}} \text{erfc} \left( \frac{-x}{\sqrt{4D(\bar{\rho})T}} \right) \right]^2 \quad (\text{S49})$$

Performing the integral yields the final result

$$\text{Var}[X(T)] = \Delta X_{\text{noise}}^2(T) + \frac{\alpha_{ic}}{\bar{\rho}} (\sqrt{2} - 1) \sqrt{\frac{2D(\bar{\rho})T}{\pi}}. \quad (\text{S50})$$

from which we identify (see (25) of the main text)

$$\Delta X_{\text{dens}}^2(T) = \frac{\sqrt{2} - 1}{\bar{\rho}} \sqrt{\frac{2D(\bar{\rho})T}{\pi}} \quad (\text{S51})$$

and hence

$$\text{Var}[X(T)] = \Delta X_{\text{noise}}^2(T) + \alpha_{ic} \Delta X_{\text{dens}}^2(T), \quad (\text{S52})$$

as given in (3) of the main text.

- [2] P. M. Chaikin and T. C. Lubensky, *Principles of Condensed Matter Physics*, Cambridge University Press, Cambridge (2013).
- [3] J. S. Bell, Phys. Rev. **129**, 1896 (1963) .
- [4] K. Malakar et al, J. Stat. Mech. (2018) 043215.
- [5] T. Demaerel and C. Maes, Phys. Rev. E **97**, 032604 (2018).
- [6] D. Martin *et al*, Phys. Rev. E **103**, 032607 (2021).
- [7] U. Basu, S. N. Majumdar, A. Rosso and G. Schehr, Phys. Rev. E **98**, 062121 (2018).
- [8] C. Bechinger, R. Di Leonardo, H. Löwen, C. Reichhardt, G. Volpe, and G. Volpe, Rev. Mod. Phys. **88**, 045006 (2016).
- [9] C. Hegde, S. Sabhapandit and A. Dhar 2014 Phys. Rev. Lett. **113**, 120601 (2014).
- [10] L. Bertini, A. De Sole, D. Gabrielli, G. Jona-Lasinio and C. Landim, Rev. Mod. Phys. **87**, 593 (2015).
- [11] B. Derrida, J. Stat. Mech. (**2011**) P01030; B. Derrida, J. Stat. Mech. (**2007**) P07023.